

S. Battisti, M. Bell, J.P. Delahaye, A. Krusche, H. Kugler, J.H.B. Madsen, A. Poncet  
CERN, Geneva, Switzerland

Summary

The EPA's purpose is to accumulate the e<sup>-</sup> and e<sup>+</sup> beam pulses from the linac into a small number (8 or 4) of bunches and it thus acts as a buffer between the fast cycling linac (100 Hz) and the slow cycling PS and SPS.

The EPA lattice design<sup>1</sup> has been completed with a number of studies described in this paper. A particle tracking through the EPA bending magnets appeared to be necessary for the final design of the structure. Studies on the dynamic aperture showed the need to remove the sextupole component in the bending magnets. The in/ejection scheme specified favours an economical hardware design. Other systems briefly described are: the vacuum, the rf and beam diagnostics.

1. Introduction

The LEP injection chain<sup>2</sup> will run in sequence with PS and SPS proton cycles. Four electron/positron cycles will take place during one PS/SPS supercycle lasting 15.12 s. The positrons are accumulated in the EPA during 11.2 s. The accumulated bunches are then used to feed two consecutive positron cycles in the PS (see chapter 5, this paper). The intensity of the e<sup>-</sup> linac beam permits the accumulation to the required bunch intensity in a short time : 1.14 s and each e<sup>-</sup> cycle in the PS is fed by one e<sup>-</sup> accumulation sequence in the EPA. The EPA operates at 600 MeV but an operating range between 500 and 650 MeV is aimed at. At first, the EPA design was based on four bunches. However, the bunch intensity required to achieve with four bunches a filling time of 12 min. for the nominal LEP current of 3mA per beam, appears to be too high to stay clear of longitudinal single-bunch instabilities and to avoid beam losses at injection in the SPS. Therefore, it was decided to base the operation on eight bunches in the EPA, PS and SPS.

2. The Structure

The EPA lattice is based on two different cells matched together and adapted respectively to the straight and to the curved part of the ring. Each one of these cells is of the quadruplet FDDF type. Many of the EPA parameters depend on the characteristics of the bending magnet. The hard edge approximation with which they were first deduced has been deemed insufficient because of the very small bending radius ( $\rho = 1.43$  m) in a specially short ( $l_m = 0.56$  m) and combined function ( $dB_y/dx = -1$  T/m) magnet. In fact, in this extreme case, the analytical integration of the exact equation of motion of the particle is not possible because of the magnetic field varying both in magnitude and gradient all along the trajectory. It is then of motion of the particle has been launched. It the reason why, in order to remove any approximation, a precise particle tracking based on the exact equation of motion of the particle has been launched. It used magnetic field estimations deduced from two dimensional computer programs whose results have been first checked by comparison with magnetic measurements on a very similar bending magnet.

The main tasks of this particle tracking was :

- a) to calculate the position of the central trajectory (Fig. 1) through the whole magnet including the fringe field extension.
- b) to adjust the total length of the magnet in order to fit the desired deflection angle.
- c) to determine the exact synchrotron integrals all along the central trajectory from the known values of

- the magnetic field and of its gradient at each point.
- d) to adjust the internal gradient in the magnet in order that the corresponding transfer matrix perturbs as little as possible the EPA lattice.
- e) to deduce the exact equivalent transfer matrix respectively in the horizontal and vertical planes, by tracking particles slightly deviated from the central orbit, and by comparing the coordinates at the entry and exit of the magnet.

After calculations with different field configurations, a new set of characteristics for the EPA bending magnet have been decided for a minimum of perturbation of the main lattice parameters. The main modification consists in a 12% increase of the internal gradient to compensate the loss in focussing by the edges due to the varying magnetic length with position. The lattice has then finally been optimised, using in place of the bending magnet, the calculated equivalent transfer matrix, by slightly adjusting the strength of the lattice and trimming quadrupoles.

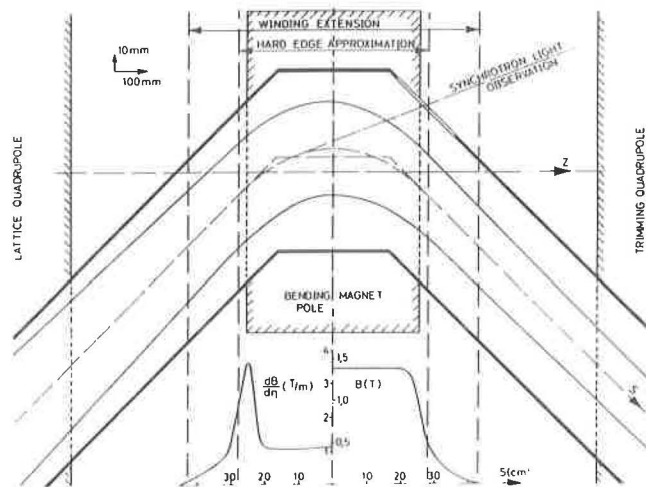


Fig. 1. Central trajectory and max beam envelope in the EPA bending magnet computed from calculated magnetic field B and orthogonal gradient dB/dn.

3. The Aperture of the Vacuum Chamber

The aperture is determined by the beam envelope at injection. The amplitudes of the betatron oscillations are kept small by the strong horizontal damping and by the relatively low values of  $\beta_{max}$ .

$$\begin{aligned} \epsilon_{xinj} < 119 \pi \mu\text{radm} & \quad \beta_x < 14.9 \text{ m} \rightarrow \sigma_{xinj} < 84 \text{ mm} \\ \epsilon_{yinj} < 10 \pi \mu\text{radm} & \quad \beta_y < 14.3 \text{ m} \rightarrow \sigma_{yinj} < 24 \text{ mm} \end{aligned}$$

The large momentum dispersion of the Linac beam ( $\Delta p/p \approx \pm 1\%$ ) does not influence the beam dimension in the injection and ejection straight sections as the dispersion function is made zero in these sections. In the curved parts of the accumulator, where the dispersion is high ( $D_x = 2.3$  m), the rms added contribution of horizontal and betatron oscillations does not exceed the value found with  $\beta_{xmax}$  only. Field tolerances of the bending magnets, alignment errors of quadrupole and bending magnets and tilts lead to closed orbit distortions of the order of  $\pm 10$ mm horizontally and  $\pm 6$  mm vertically. With these orbit distortions

tions, the beam stays within the vacuum chamber aperture fixed at:  $\varnothing_x = 100$  mm and  $\varnothing_y = 35$  mm. In the long straight sections a round chamber  $\varnothing = 100$  mm will be used (see also Fig. 2).

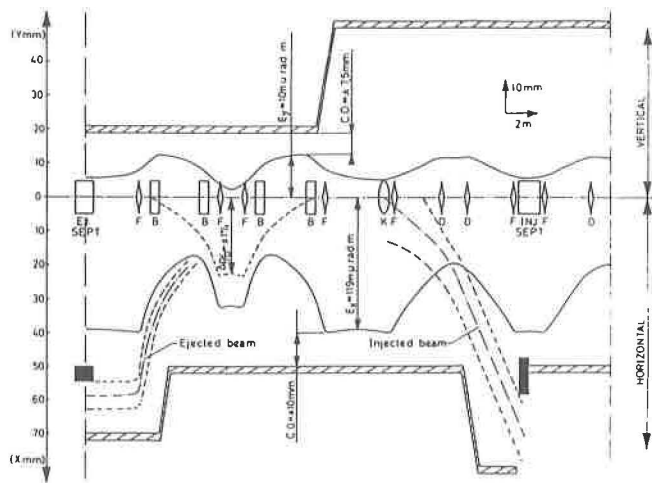


Fig. 2. Max horizontal and vertical beam envelope at injection inside the vacuum chamber along a quarter of the EPA ring (half a superperiod).

#### 4. The pinch effect on the dynamic aperture due to the sextupole component in the bending magnets

Following Parzen's empirical formulae<sup>3</sup> the sextupole component in the EPA bending magnet should be between -3 and -5.5 T/m. This component increases the non-linearities in the machine and has thus an influence on the dynamic aperture. The program Patricia<sup>4</sup> has been used to track particles through the lattice including - attached to the bending magnets - sextupoles of various strengths. The results of the tracking runs are summarized in Fig. 3. This figure shows the quarter of a vertical cut through the particle path at the beginning of the lattice. Particles with different magnitude of  $\sigma_x$  and ratio's  $\sigma_x/\sigma_y$  have been tracked with four different sextupole forces (0, -2.8, -4.8, -7.2 T/m) at the bending magnets. The particles do 1000 turns and undergo during that time 2 synchrotron oscillations with a momentum swing of  $\pm 1.2$  %. The curves locate the borders of the dynamic aperture as function of the sextupole forces. Survival of 1000 turns does not necessarily mean that the particle rests stable. As can be seen in the phase space plots and frequency spectra provided by Patricia, coupling of betatron-synchrotron oscillations show up at the borders and locking in of particles at resonances cannot be excluded. To keep the dynamic aperture large it has therefore been decided to compensate the sextupole component after measurement of the first magnet by adding shims at the end-faces.

#### 5. The In/Ejections

A pair of fast injection kickers and a pair of slow orbit bumpers give a local orbit displacement having its max at the injection septum. The accumulation of the Linac pulses takes place in the betatron phase plane close to the stored bunch and is done at an equal rate in each of the eight equidistant circulating bunches. The distance between the bunch center is 52.4 ns and the bunch length at max 25 ns. A delay line type kicker with the required short rise time will be used. The Linac pulses, rep. frequency 100 Hz, are injected by a configuration of 2 conventional dc septum magnets ( $7.25^\circ$  and  $21.75^\circ$ ) with 11 mm septum width.

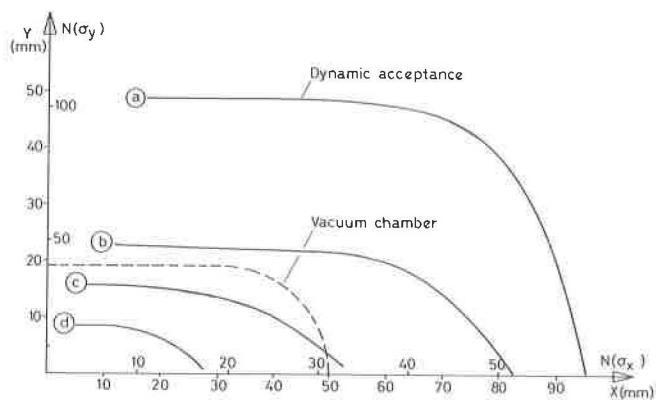


Fig. 3. Restriction of the EPA dynamic aperture with the sextupole component of the bending magnet at a) 0T/m, b) -2.8 T/m, c) -4.8 T/m and d) -7.2 T/m.

The EPA circumference (125.7 m) is exactly one fifth of the PS to achieve a beam transfer within one PS turn. For the fast ejection of the  $e^+$  and  $e^-$  bunches a common ejection septum magnet (ac) and kicker system is used. An arrangement of four thyratrons pulsed in series in a short delay line magnet module will be used<sup>5</sup>. Two such systems provide then the required eight kicks within 2.1  $\mu\text{s}$ .

To reduce the charge of the ejected  $e^+$  bunches by half, a cutting ejection will be used. The principle of this process is shown in Fig. 4.

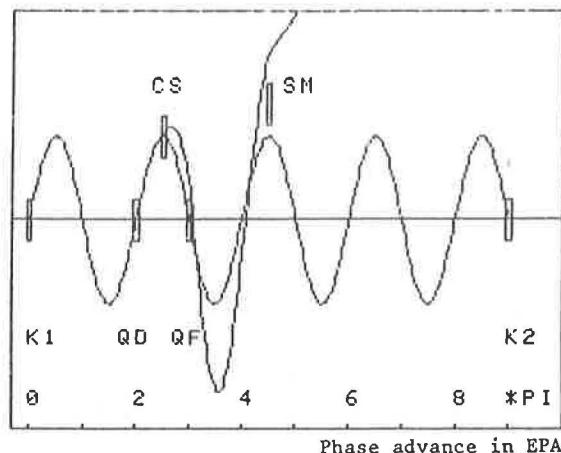


Fig. 4. Principle and trajectories of cutting ejection

The fast kicker (K1) positions the beam at the cutting septum (CS). The part of the beam, which did not see a deflection of the CS, oscillates without being extracted until the oscillation is stopped by a second kicker system (K2). A matched quadrupole pair QD and QF, spaced by  $\pi$  phase advance in both planes in the  $90^\circ$  lattice cell of EPA provides two functions: i) the horizontal  $\beta$ -function at CS is increased from 14 m to up to 120 m which produces a reduction in the systematic beam loss, ii) the part of the beam deflected by the CS receives by the QF a favourable phase shift and kick enhancement which separates the beam at the ejection septum SM.

#### 6. The Radio-Frequency

The rf parameters are selected for achieving a longitudinally stable beam transfer from the EPA to the PS<sup>6</sup>. Furthermore, during accumulation the half-bucket

height  $\Delta_b$  will be sufficient to accept the linac beam. Since the  $e^+$  beam has a spread of  $\pm 1\%$  we imposed  $\Delta_b > 1.2\%$ . The lowest possible harmonic number (8) is chosen and the corresponding frequency is 19.085 MHz. A peak voltage of 50 kV will be used during accumulation and ejection.

### 7. The Vacuum

With an average gas pressure of  $10^{-8}$  Torr, the beam life time will be sufficiently large (in excess of several minutes). An average pressure in the vacuum chamber of  $10^{-8}$  Torr, with beam, can be obtained in a non-in-situ-bakeable system (except for a few high degassing components). The main problem due to the interaction of  $e^-$  with the residual gas molecules results from the creation and trapping of ions by the circulating bunches. At  $10^{-8}$  Torr with 50%  $H_2$  and 50% composed of  $H_2O$ ,  $CO$ ,  $CH_4$ ,  $CO_2$ , it takes on the average 0.15 s for each circulating electron to produce an ion i.e. to reach full neutralization in the absence of any clearing mechanism. With 8 bunches of length  $6\tau_s = 1.2$  m, and total intensity of  $10^{11} e^+$ , an incoherent space charge Q-shift of 0.14 would occur, value unacceptably high. A gas pressure of  $10^{-10}$  Torr would probably not be sufficient to avoid possible harmful effects due to ion trapping. The vacuum system design aims to achieve  $10^{-8}$  Torr with beam, about  $5 \cdot 10^{-9}$  Torr without beam. To solve the ion trapping problem, several ion clearing possibilities have been examined such as creating beam closed orbit distortions. However the only way to remove the ions without any beam disturbance, is to use ion clearing electrodes. The pumping ports of the ion pumps of the vacuum chamber are a convenient location for inserting a grid which can be polarized with a negative voltage eventually drawn from the triode's own power supply. In the bending sections ion pumps are located at about 3 m interval and at both ends of the bending magnets. Calculations show that with the clearing grids, the beam neutralization can be reduced by a factor of at least 10.

### 8. Beam Diagnostics

To find the beam emittance and the phase plane ellipse at the outlet of the linac wire scanners will be used to measure the transverse beam profiles. For matching the beam at injection in EPA, wire scanners are used again. The trajectory of the injected bunch and the closed orbit will be measured with magnetic type position detectors. The magnetic type was chosen as it satisfies the sensitivity and the bandwidth required (150 kHz to 50 MHz). The detector enables us to measure the bunch charge as well, and has the advantage of being little affected by particle losses. It is physically short and relatively cheap. The transverse and the longitudinal beam profiles will be observed with a synchrotron radiation light beam in the visible wave length. The light beam will be guided to the equipment building next to the EPA and analyzed there.

### 9. Conclusion and Status

The EPA is a dedicated machine in the LEP injection chain. Its design favours an efficient and economical injection/accumulation and ejection/transfer process. The studies showed that the accumulator design requires careful considerations of the beam optics in the short bending magnets with their low bending radius.

One of the next steps in the design will be the definition of the different control functions and their parameters. The controls of EPA will be integrated in the new PS control system.

The civil engineering work will be finished in spring 84 and the first beam accumulation is expected two years later.

### References

1. J.P. Delahaye and A. Krusche. "The lattice design of the LEP Electron Positron Accumulator (EPA)", Part. Acc. Conf (1983) Santa Fe, NM.
2. LEP Injector Study Group. "The chain of LEP Injectors", Part. Acc. Conf. (1983) Santa Fe, NM.
3. G. Parzen, ISA 76-13, BNL (1976).
4. H. Wiedemann, Technical Memo PTM-230 (1981).
5. D. Grier and K.D. Metzmacher. IEEE Pulsed Power Conf., Albuquerque, NM (1983).
6. K. Hübner and J.H.B. Madsen, LEP Note 378 (1982).

TABLE 1

#### General

Circumference	C	= 125.66	m
Nominal working energy	E	= 600	MeV/c
Number of bunches	k	= 8/4	--
Nominal charge per bunch	N/k	= $2.5 \cdot 10^{10}$	$e^\pm$

#### Beam parameters at injection

Maximum emittances	$\epsilon_x; \epsilon_y$	= 119;10	$\mu\text{radm}$
Momentum dispersion	$\Delta p/p$	= $\pm 1$	$10^{-2}$
Bunch length	L	= 12 - 25	ns

#### Beam parameters at equilibrium ( $\pm 1\sigma$ )

Transverse emittances	$\epsilon_{x0}; \epsilon_{y0}$	= 0.135;0.027	$\mu\text{radm}$
Momentum dispersion	$q_E/E$	= $\pm 6.0$	$10^{-4}$
Bunch length	$\sigma_s$	= 21.0	cm

#### Lattice

Superperiodicity	2
Half of one superperiod	1/2(arc)-1/2(straight)
Half of arc	FBBF FBBF
Half of straight section	FDDF FD
Betatron tune	$Q_x; Q_y$ = 4.45;4.38
Transition Energy	$\gamma_{tr}$ = 5.52
Natural chromaticities	$\xi_x; \xi_y$ = -1.11;-2.60

#### Synchrotron radiation and damping

Energy loss per turn	$U_Y$	= 7.21	keV
Damping partition number	$J_x; J_y; J_z$	= 2;1;1	
Damping time constants	$\tau_x; \tau_y; \tau_z$	= 34;70;70	ms

Main ring elements	Number	Strength	Observations
Bending magnets	16	0.7846 Tm 0.5452 T	Straight $\rho = 1.43$ m
Quadrupole magnets	40	< 1 T	4 families
Sextupole magnets	12	< 7.5 T/m	2 families
Injection septa	2	0.76 Tm	dc outside
	2	0.25 Tm	vacuum
Ejection septum	1	0.47 Tm	ac
Injection kickers	4	41 Gm	pulsed 100Hz
Ejection kickers	2	29 Gm	8 pulses
RF cavity	1	h=8 f=19.1MHz	$V_{RF} < 50$ kV